

Timelike Compton Scattering - new theoretical results and experimental possibilities

Jakub Wagner

Theoretical Physics Department
National Center for Nuclear Research, Warsaw

DIS2012, March 29th

in collaboration with

B. Pire (CPhT Ecole Polytechnique, Palaiseau) L. Szymanowski (NCNR, Warsaw) H. Moutarde and F. Sabatie (CEA, Saclay)

Outline

- 1 Timelike Compton Scattering - Introduction
- 2 Basic properties of TCS, first experimental results
- 3 TCS at NLO
- 4 Ultraperipheral collisions

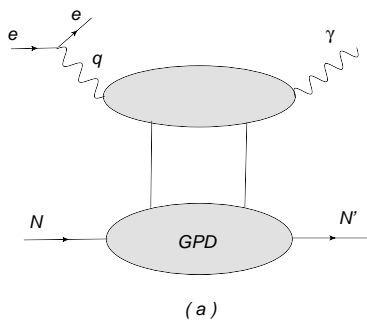


Figure: Deeply Virtual Compton Scattering : $lN \rightarrow l'N'\gamma$

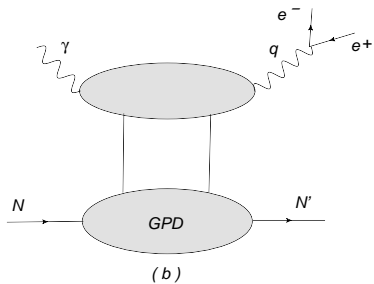


Figure: Timelike Compton Scattering: $\gamma N \rightarrow l^+ l^- N'$

Why TCS?

- GPDs enter factorization theorems for hard exclusive reactions (DVCS, deeply virtual meson production, TCS etc.), in a similar manner as PDFs enter factorization theorem for DIS
- First moment of GPDs enters the Ji's sum rule for the angular momentum carried by partons in the nucleon,
- Deeply Virtual Compton Scattering (DVCS) is a golden channel for GPDs extraction,
- Why TCS: universality of the GPDs, another source for GPDs (special sensitivity on real part), spacelike-timelike crossing and understanding the structure of the NLO corrections,
- Experiments *at low energy*: CLAS 6 GeV \rightarrow CLAS 12 GeV, *at high energy*: RHIC, LHC ?

Coordinates

Berger, Diehl, Pire, 2002

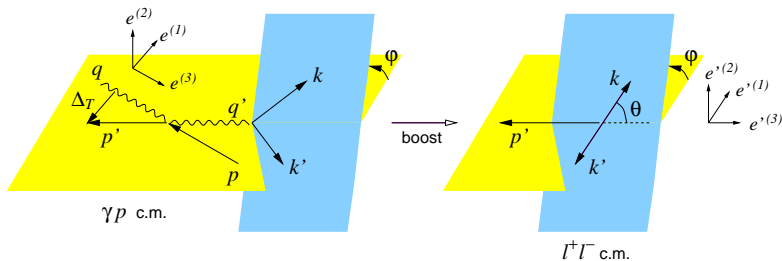


Figure: Kinematical variables and coordinate axes in the γp and $l^+ l^-$ c.m. frames.

The Bethe-Heitler contribution

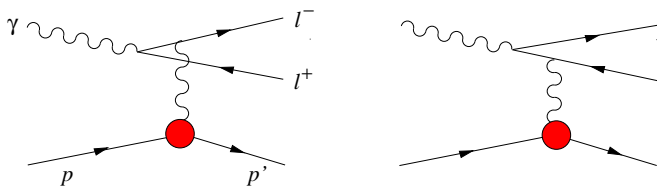


Figure: The Feynman diagrams for the Bethe-Heitler amplitude.

$$\frac{d\sigma_{BH}}{dQ'^2 dt d\cos\theta} \approx 2\alpha^3 \frac{1}{-tQ'^4} \frac{1 + \cos^2\theta}{1 - \cos^2\theta} \left(F_1(t)^2 - \frac{t}{4M_p^2} F_2(t)^2 \right),$$

For small θ BH contribution becomes very large

The Compton contribution

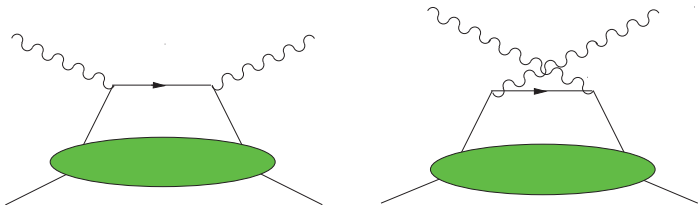


Figure: Handbag diagrams for the Compton process in the scaling limit.

$$\frac{d\sigma_{TCS}}{dQ'^2 d\Omega dt} \approx \frac{\alpha^3}{8\pi} \frac{1}{s^2} \frac{1}{Q'^2} \left(\frac{1 + \cos^2 \theta}{4} \right) 2(1 - \xi^2) |\mathcal{H}(\xi, t)|^2,$$

$$\mathcal{H}(\xi, t) = \sum_q e_q^2 \int_{-1}^1 dx T(x, \xi, Q') H^q(x, \xi, t),$$

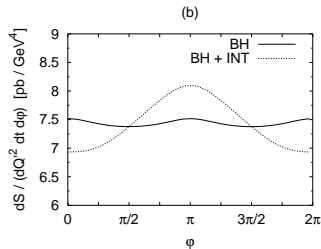
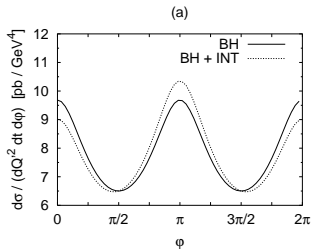
Interference

The interference part of the cross-section for $\gamma p \rightarrow l^+ l^- p$ with unpolarized protons and photons is given at leading order by

$$\frac{d\sigma_{INT}}{dQ^2 dt d\cos\theta d\varphi} \sim \cos\varphi \operatorname{Re}\mathcal{H}(\xi, t)$$

Linear in GPD's, odd under exchange of the l^+ and l^- momenta \Rightarrow angular distribution of lepton pairs is a good tool to study interference term.

Berger, Diehl, Pire, 2002



B-H dominant for small energies;

JLAB 6 GeV data

Rafael Paredes PhD thesis

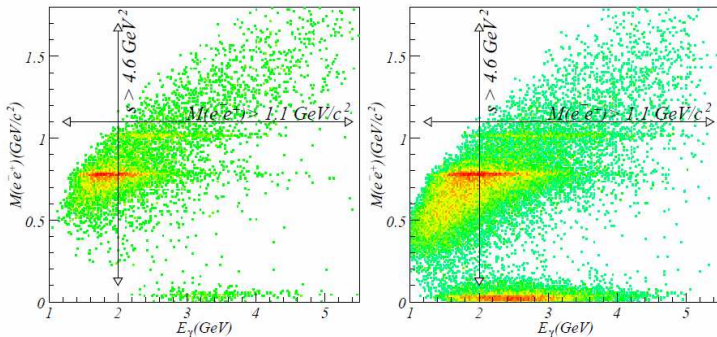


Figure: e^+e^- invariant mass distribution vs quasi-real photon energy. For TCS analysis $M(e^+e^-) > 1.1 \text{ GeV}$ and $s_{\gamma p} > 4.6 \text{ GeV}^2$ regions are chosen. Left graph represents e1-6 data set, right one is from e1f data set.

There is more data from g12 data set, soon to be analyzed. 12 GeV upgrade enables exploration of invariant masses up to $Q^2 = 9 \text{ GeV}^2$ mass.

Theory vs experiment

R.Paremuzyan and V.Guzey:

$$R = \frac{\int d\phi \cos\phi d\sigma}{\int d\phi d\sigma}$$

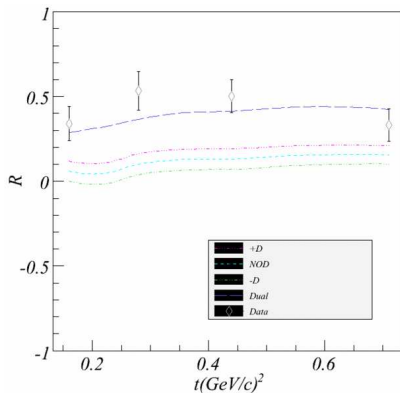


Figure: Theoretical prediction of the ratio R for various GPDs models. Data points after combining both e1-6 and e1f data sets.

Motivation for NLO

Why do we need NLO corrections to TCS:

- gluons enter at NLO,
- DIS versus Drell-Yan: big K-factors
- reliability of the results, factorization scale dependence,

$$\log \frac{-Q^2}{\mu_F^2} \rightarrow \log \frac{Q^2}{\mu_F^2} \pm i\pi,$$

Belitsky, Mueller, Niedermeier, Schafer, Phys.Lett.B474 ,2000.

Pire, Szymanowski, Wagner, Phys.Rev.D83, 2011.

General Compton Scattering:

$$\gamma^*(q_{in})N \rightarrow \gamma^*(q_{out})N'$$

- DVCS: $q_{in}^2 < 0$, $q_{out}^2 = 0$
- TCS: $q_{in}^2 = 0$, $q_{out}^2 > 0$
- DDVCS: $q_{in}^2 < 0$, $q_{out}^2 > 0$

Amplitude:

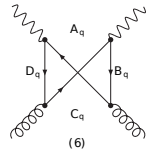
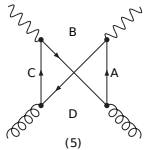
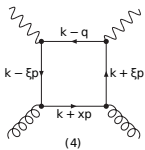
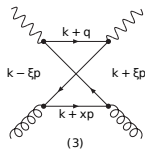
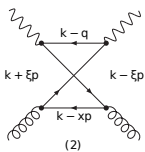
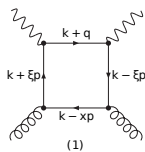
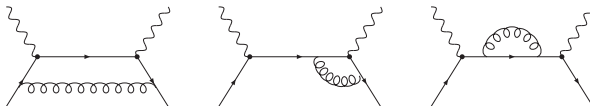
$$\mathcal{A}^{\mu\nu} = g_T^{\mu\nu} \int_{-1}^1 dx \left[\sum_q^{n_F} T^q(x) F^q(x) + T^g(x) F^g(x) \right]$$

where renormalized coefficient functions are given by:

$$T^q = C_0^q + C_1^q + \ln\left(\frac{Q^2}{\mu_F^2}\right) \cdot C_{coll}^q,$$

$$T^g = C_1^g + \ln\left(\frac{Q^2}{\mu_F^2}\right) \cdot C_{coll}^g$$

Diagrams



Results: TCS + DVCS + DDVCS

TCS:

Quark coefficient functions:

$$C_0^q = e_q^2 \left(\frac{1}{x - \xi - i\varepsilon} + \frac{1}{x + \xi + i\varepsilon} \right),$$

$$C_1^q = \frac{e_q^2 \alpha_S C_F}{4\pi}$$

$$\left\{ \frac{1}{x - \xi - i\varepsilon} \left[-9 + 3 \log\left(-1 + \frac{x}{\xi} - i\varepsilon\right) - 6 \frac{\xi}{x + \xi} \log\left(-1 + \frac{x}{\xi} - i\varepsilon\right) + 6 \frac{\xi}{x + \xi} \log(-2 - i\varepsilon) \right. \right. \\ \left. \left. + \log^2\left(-1 + \frac{x}{\xi} - i\varepsilon\right) - \log^2(-2 - i\varepsilon) \right] \right. \\ \left. + \frac{1}{x + \xi + i\varepsilon} \left[-9 + 3 \log\left(-1 - \frac{x}{\xi} - i\varepsilon\right) + 6 \frac{\xi}{x - \xi} \log\left(-1 - \frac{x}{\xi} - i\varepsilon\right) - 6 \frac{\xi}{x - \xi} \log(-2 - i\varepsilon) \right. \right. \\ \left. \left. + \log^2\left(-1 - \frac{x}{\xi} - i\varepsilon\right) - \log^2(-2 - i\varepsilon) \right] \right\},$$

$$C_{coll}^q = \frac{e_q^2 \alpha_S C_F}{4\pi} \left\{ \frac{1}{x - \xi - i\varepsilon} \left[3 + 2 \log\left(-1 + \frac{x}{\xi} - i\varepsilon\right) - 2 \log(-2 - i\varepsilon) \right] \right. \\ \left. + \frac{1}{x + \xi + i\varepsilon} \left[3 + 2 \log\left(-1 - \frac{x}{\xi} - i\varepsilon\right) - 2 \log(-2 - i\varepsilon) \right] \right\}$$

Gluon coefficient functions:

$$C_{coll}^g = \frac{\left(\sum_q e_q^2\right) \alpha_S T_F}{4\pi} \frac{2}{(x + \xi + i\varepsilon)(x - \xi - i\varepsilon)} \cdot$$

$$\left[\frac{x - \xi}{x + \xi} \log\left(-1 + \frac{x}{\xi} - i\varepsilon\right) + \frac{x + \xi}{x - \xi} \log\left(-1 - \frac{x}{\xi} - i\varepsilon\right) - 2 \frac{x^2 + \xi^2}{x^2 - \xi^2} \log(-2 - i\varepsilon) \right],$$

$$C_1^g = \frac{\left(\sum_q e_q^2\right) \alpha_S T_F}{4\pi} \frac{1}{(x + \xi + i\varepsilon)(x - \xi - i\varepsilon)} \cdot$$

$$\left[-2 \frac{x - 3\xi}{x + \xi} \log\left(-1 + \frac{x}{\xi} - i\varepsilon\right) + \frac{x - \xi}{x + \xi} \log^2\left(-1 + \frac{x}{\xi} - i\varepsilon\right) \right.$$

$$- 2 \frac{x + 3\xi}{x - \xi} \log\left(-1 - \frac{x}{\xi} - i\varepsilon\right) + \frac{x + \xi}{x - \xi} \log^2\left(-1 - \frac{x}{\xi} - i\varepsilon\right)$$

$$\left. + 4 \frac{x^2 + 3\xi^2}{x^2 - \xi^2} \log(-2 - i\varepsilon) - 2 \frac{x^2 + \xi^2}{x^2 - \xi^2} \log^2(-2 - i\varepsilon) \right]$$

Discussion

The result may be summarized as follows:

$$\xi_D = \xi - i\epsilon \quad \xi_T = \xi + i\epsilon$$

$$\begin{aligned} {}^T C_0^q &= C_0^q(x, \xi_T) = C_0^q(x, \xi_D^*) = {}^D C_0^{q*} \\ {}^T C_{coll}^q &= C_{coll}^q(x, \xi_T) = C_{coll}^q(x, \xi_D^*) = {}^D C_{coll}^{q*} \\ {}^T C_1^q &= C_1^q(x, \xi_T) - i\pi C_{coll}^q(x, \xi_T) = {}^D C_1^{q*} - i\pi {}^D C_{coll}^{q*}, \end{aligned}$$

for the quark contributions and

$$\begin{aligned} {}^T C_{coll}^g &= C_{coll}^g(x, \xi_T) = C_{coll}^g(x, \xi_D^*) = {}^D C_{coll}^{g*} \\ {}^T C_1^g &= C_1^g(x, \xi_T) - i\pi C_{coll}^g(x, \xi_T) = {}^D C_1^{g*} - i\pi {}^D C_{coll}^{g*} \end{aligned}$$

for the gluonic contribution. The above relations lead to the following relations between the complete coefficient functions:

$${}^T T^q = {}^D T^{q*} - i\pi {}^D C_{coll}^{q*} \quad {}^T T^g = {}^D T^{g*} - i\pi {}^D C_{coll}^{g*}.$$

DVCS Compton Form Factors at NLO

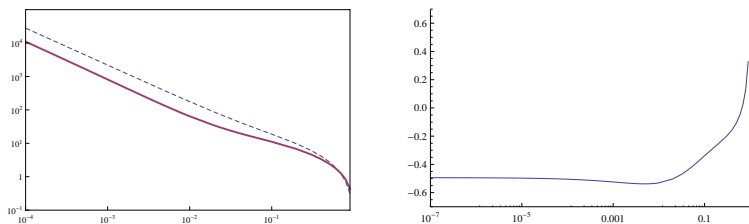


Figure: (left) Imaginary part of the DVCS Compton Form Factor \mathcal{H} , in the LO (dashed) and NLO (solid). (right) Ratio of the NLO correction to the Born term for imaginary part of the Compton Form Factor \mathcal{H} . Calculated for Kroll-Goloskokov model with $t = -0.1 \text{ GeV}^2$, $Q^2 = 5 \text{ GeV}^2$.

see previous H.Moutarde talk

TCS Compton Form Factors at NLO

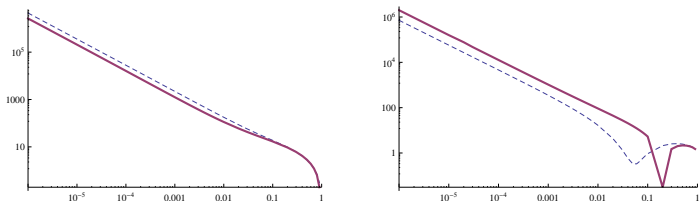


Figure: (left) Absolute value of the imaginary part of the TCS Compton Form Factor \mathcal{H} , in the LO (dashed) and NLO (solid). (right) Absolute value of the real part of the TCS Compton Form Factor \mathcal{H} , in the LO (dashed) and NLO (solid). Calculated for Kroll-Goloskokov model with $t = -0.1 \text{ GeV}^2$, $Q^2 = 5 \text{ GeV}^2$.

TCS Compton Form Factors at NLO

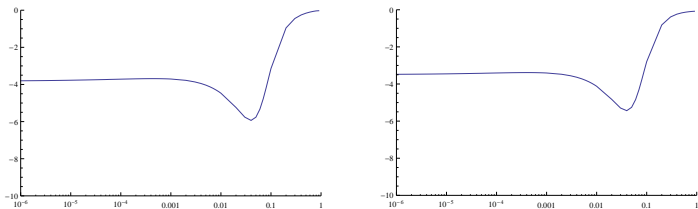


Figure: (left) Ratio of the NLO correction to the Born term for the **real** part of CFF \mathcal{H} . (right) Gluon contribution to that ratio.

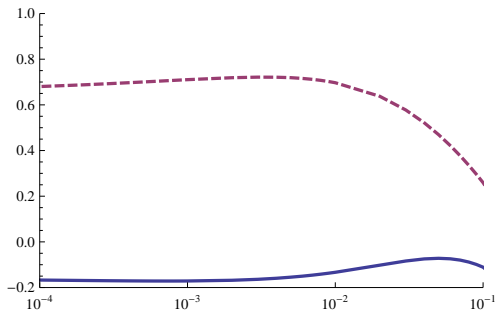
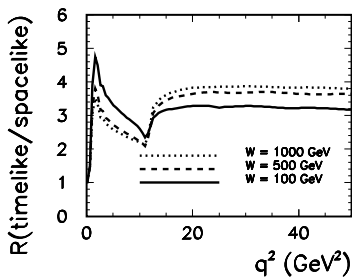


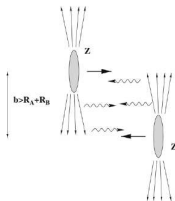
Figure: Ratio of the real to imaginary part of the TCS Compton Form Factor \mathcal{H} in the LO (solid) and NLO (dashed).

Interesting result in k_T factorization:

W. Schafer, G. Slipek, A. Szczurek, Phys.Lett.B688:185-191,2010.



Ultraperipheral collisions



$$\sigma_{pp} = 2 \int \frac{dn(k)}{dk} \sigma_{\gamma p}(k) dk$$

$\sigma_{\gamma p}(k)$ is the cross section for the $\gamma p \rightarrow pl^+l^-$ process and k is the γ 's energy, and $\frac{dn(k)}{dk}$ is an equivalent photon flux.

For $\theta = [\pi/4, 3\pi/4]$, $\phi = [0, 2\pi]$, $t = [-0.05 \text{ GeV}^2, -0.25 \text{ GeV}^2]$, $Q'^2 = [4.5 \text{ GeV}^2, 5.5 \text{ GeV}^2]$, and photon energies $k = [20, 900] \text{ GeV}$ we get:

$$\sigma_{pp}^{BH} = 2.9 \text{ pb} .$$

The Compton contribution gives:

$$\sigma_{pp}^{TCS} = 1.9 \text{ pb} .$$

The interference cross section

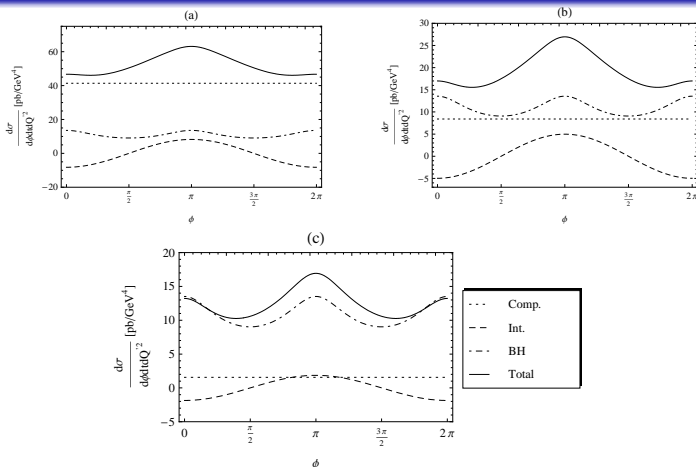


Figure: The differential cross sections (solid lines) for $t = -0.2 \text{ GeV}^2$, $Q'^2 = 5 \text{ GeV}^2$ and integrated over $\theta = [\pi/4, 3\pi/4]$, as a function of φ , for $s = 10^7 \text{ GeV}^2$ (a), $s = 10^5 \text{ GeV}^2$ (b), $s = 10^3 \text{ GeV}^2$ (c) with $\mu_F^2 = 5 \text{ GeV}^2$. We also display the Compton (dotted), Bethe-Heitler (dash-dotted) and Interference (dashed) contributions.

Ultraperipheral collisions at RHIC

$$L \cdot k \frac{dn}{dk} (\text{mb}^{-1} \text{sec}^{-1})$$

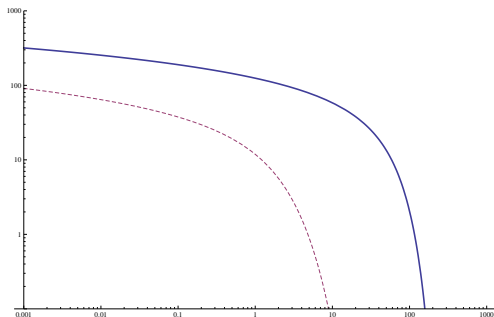


Figure: Effective luminosity of the photon flux from the Au-Au (dashed) and proton-proton (solid) collisions as a function of photon energy k (GeV).

$$\frac{d\sigma^{AuAu}}{dQ^2 dt d\phi} (\mu\text{b GeV}^{-4})$$

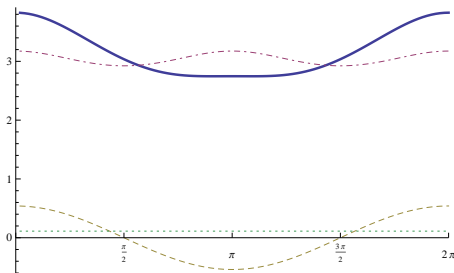


Figure: The differential cross sections (solid lines) for $t = -0.1 \text{ GeV}^2$, $Q'^2 = 5 \text{ GeV}^2$ and integrated over $\theta = [\pi/4, 3\pi/4]$, as a function of ϕ . We also display the Compton (dotted), Bethe-Heitler (dash-dotted) and Interference (dashed) contributions.

Total BH cross section (for $Q \in (2, 2.9) \text{ GeV}$, $t \in (-0.2, -0.05) \text{ GeV}^2$, $\theta = [\pi/4, 3\pi/4]$ and $\phi \in (0, 2\pi)$)

$$\sigma_{BH} = 41 \mu\text{b}$$

$$\text{Rate} = 0.04 \text{ Hz}$$

$$\frac{d\sigma^{PP}}{dQ^2 dt d\phi} (\text{pb GeV}^{-4})$$

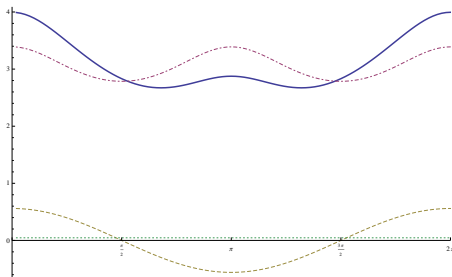


Figure: The differential cross sections (solid lines) for $t = -0.1 \text{ GeV}^2$, $Q'^2 = 5 \text{ GeV}^2$ and integrated over $\theta = [\pi/4, 3\pi/4]$, as a function of ϕ . We also display the Compton (dotted), Bethe-Heitler (dash-dotted) and Interference (dashed) contributions.

Total BH cross section (for $Q \in (2, 2.9) \text{ GeV}$, $t \in (-0.2, -0.05) \text{ GeV}^2$, $\theta = [\pi/4, 3\pi/4]$ and $\phi \in (0, 2\pi)$)

$$\sigma_{BH} = 9\text{pb} \quad \text{Rate} = 5/\text{day}$$

Summary

- TCS already measured in JLAB 6 GeV, but much richer and more interesting kinematical region available after upgrade to 12 GeV.
- Big NLO corrections from gluon sector,
- Better understanding of large terms (π^2 , ??) is needed - factorization scheme? resummation ?
- Compton scattering in ultraperipheral collisions at hadron colliders opens a new way to measure generalized parton distributions - experimentally challenging.